ORIGINAL ARTICLE

Importance of estimation of optimum isotherm model parameters for adsorption of methylene blue onto biomass derived activated carbons: Comparison between linear and non-linear methods

Paidinaidu Paluri [1] · Khwaja Alamgir Ahmad [1] · Krishna Sandilya Durbha [1]

Abstract

A comparison of the linear and non-linear methods for the selection of optimum equilibrium isotherm for the adsorption of methylene blue onto the banana root (*Musa acuminata*) derived activated carbons was carried out. The adsorption equilibrium data were fitted to three isotherm models: Langmuir, Freundlich, and Temkin. The prediction of optimum isotherm was based on six error functions: the coefficient of determination (R^2), the sum of the squares of the errors (SSE), the sum of the absolute errors (SAE), the average relative error (ARE), the hybrid fractional error function (HYBRID), and the Marquardt's percent standard deviation (MPSD). The optimum isotherm achieved was the Temkin isotherm in non-linear and linear form followed by Freundlich and Langmuir based on the error functions. Non-linear pseudo-first-order and pseudo-second-order kinetic models analyzed the adsorption data. The present work demonstrated that the non-linear method is a more suitable method to estimate the isotherm parameters than the linear method, and the pseudo-first-order model best fitted the corresponding experimental data.

Keywords Banana root · Activated carbon · Methylene blue · Non-linear isotherms · Kinetics · Error functions

1 Introduction

Water pollution due to an effluent dye is identified as one of the most primary hazards that is produced by wastes of cosmetics, dye manufacturing industries, food processing, leather, and textile industries due to its characteristics [1–3]. Methylene blue (MB), the most common effluent found in the textile industry, is classified as a basic dye material which is widely used for dyeing of cotton, silk, and wool. Although MB is not classified as hazardous as a heavy metal pollutant, it can lead to harmful effects on human health and microorganisms due to constant exposure to an excessive quantity of this dye [4, 5].

Various methods are used to remove pollutants from wastewater, such as biological, chemical, and physical (including adsorption) purification processes [6–8]. Adsorption is the most frequently used method for the treatment of wastewater

by using activated carbon [9]. Adsorption performance and capacity of the activated carbon (AC) are generally obtained from equilibrium adsorption isotherm studies. Adsorption isotherms describe the equilibrium relationships between the adsorbate and the adsorbent [10]. The regularly used isotherm models by numerous researchers for the adsorption are Langmuir, Freundlich, Temkin, BET, Redlich-Peterson, and Dubinin–Radushkevich isotherms, etc.

The best-fit adsorption isotherm can be found using linear regression by the method of least-squares. It is the most commonly used method for predicting the optimum isotherm [11, 12]. The difference between the model predicted values and the experimental equilibrium data is minimized by using various types of error functions [13]. The best-fit isotherm model for adsorption is selected based on the highest value of the coefficient of determination and the least value of the other error functions.

1.1 Error functions

In the present study, the coefficient of determination and five distinct kinds of error functions performed a very significant

✉ Paidinaidu Paluri
  naidu@iitism.ac.in

1 Department of Chemical Engineering, Indian Institute of Technology (Indian School of Mines), Dhanbad, Dhanbad, India

Table 1 Error functions and their corresponding equations

Error function	Equation
Coefficient of determination (R^2)	$\dfrac{\sum_{i=1}^{n}\left(q_{e,\exp}-\overline{q_{e,cal}}\right)^2}{\sum_{i=1}^{n}\left(q_{e,\exp}-\overline{q_{e,cal}}\right)^2+\sum_{i=1}^{n}\left(q_{e,\exp}-q_{e,cal}\right)^2}$
Sum of squares of the errors (SSE)	$\sum_{i=1}^{n}\left(q_{e,exp}-q_{e,cal}\right)^2$
Average relative error (ARE)	$\dfrac{100}{n}\sum_{i=1}^{n}\left|\dfrac{q_{e,exp}-q_{e,cal}}{q_{e,exp}}\right|$
Sum of the absolute errors (SAE)	$\sum_{i=1}^{n}\left|q_{e,exp}-q_{e,cal}\right|$
The hybrid fractional error function (HYBRID)	$\dfrac{100}{n-p}\sum_{i=1}^{n}\left|\dfrac{q_{e,exp}-q_{e,cal}}{q_{e,exp}}\right|$
Marquardt's percent standard deviation (MPSD)	$100\times\sqrt{\dfrac{1}{n-p}\sum_{i=1}^{n}\left(\dfrac{q_{e,exp}-q_{e,cal}}{q_{e,exp}}\right)^2}$

role in determining the optimum isotherm model and enhancing the optimization procedure for given experimental data (Table 1) [14–17].

where $q_{e,\ exp}$ and $q_{e,\ cal}$ are the experimental and calculated values of the equilibrium adsorbate concentration in the solid phase (mg/g), respectively. $\overline{q_{e,cal}}$ is the mean of the all calculated ($q_{e,\ cal}$) values, and n and p are the number of data points and parameters in the isotherm model, respectively.

Most of the adsorption isotherms proposed in the literature were non-linear models. Linearization of non-linear models to estimate the model parameter(s) may alter the error distribution. Some of the researchers have studied the comparison of linear and non-linear isotherm models for the estimation of model parameters [18–21].

In the present study, an abundantly available biomass waste was used as the raw material for the production of novel ACs. To study the effect of adsorptive properties of the ACs, impregnation ratio and carbonization temperature were varied. Three linear and non-linear isotherm models were analyzed to obtain the optimum isotherm and isotherm parameters for the adsorption of MB onto various ACs derived from the banana root. The adsorption equilibrium studies were conducted for different initial MB concentrations at three different temperatures of 25, 30, and 40 °C.

2 Materials and methods

2.1 Materials

The banana root (*Musa acuminata*) was obtained from the local farming field from Andhra Pradesh, India. The raw material was manually selected, cleaned with distilled water several times, cut into small pieces, dried at 105 °C for 24 h, and was ground thereafter using a household mixer-grinder. The ground material was screened, and the material in the particle size range of 300–425 μm was collected and stored in zip-lock plastic bags. The physical and chemical characterization of this ground raw material was carried out. All the chemicals used in the present study were of analytical grade and purchased from Merck Life Science Private Limited, India.

2.2 Preparation of activated carbons

The ground raw material was chemically activated by using zinc chloride (95% (wt.)). The weight ratio of raw material to that of zinc chloride (impregnation ratio) was varied from 1:1 to 1:4, and the corresponding amounts of zinc chloride per 10 g of raw material were 10.53, 21.05, 31.58, and 42.1 g, respectively. The raw material and zinc chloride were mixed in 300 ml of doubled distilled water, and the solution was

Table 2 Nomenclature of ACs from the banana root (BR) activated with zinc chloride

Impregnation ratio	Carbonization temperature (°C)	Sample name
1:1	400	AC-11-400
1:2		AC-12-400
1:3		AC-13-400
1:4		AC-14-400
1:1	500	AC-11-500
1:2		AC-12-500
1:3		AC-13-500
1:4		AC-14-500
1:1	600	AC-11-600
1:2		AC-12-600
1:3		AC-13-600
1:4		AC-14-600

Table 3 Linear and non-linear forms of isotherm models [21]

Types of isotherm	Non-linear expression	Linear expression	Parameters
Freundlich	$q_e = K_F C_e^{1/n}$	$\ln q_e = \ln K_F + \frac{1}{n} \ln C_e$	K_F, n
Langmuir	$q_e = \frac{Q_0 K_L C_e}{1 + K_L C_e}$	$\frac{C_e}{q_e} = \left(\frac{1}{Q_0 K_L}\right) + \frac{C_e}{Q_0}$	Q_0, K_L
Temkin	$q_e = \frac{RT}{b_T} \ln K_T \, C_e$	$q_e = \frac{RT}{b_T} \ln K_T + \frac{RT}{b_T} \ln C_e$	K_T, b_T

stirred at 450 rpm, at 85 °C for 6 h. The slurry was then filtered, and the solid residue was collected and dried at 105 °C for 24 h in an electric hot air oven. The impregnated solid was placed in an alumina crucible with a lid and kept inside the electric tubular furnace. The solid was heated to a final selected temperature ranging from 400 to 600 °C with a heating rate of 10 °C/min, and the final temperature attained was maintained for 1 h under inert (nitrogen flow) atmosphere. The solid was then allowed to cool down to room temperature. The prepared activated carbon was washed extensively with double distilled water and dried in an electric hot air oven at 105 °C until such time that the weight of the dried sample became constant. The dried sample was stored in a zip-lock plastic bag. The activated carbon (AC) samples prepared under various experimental conditions were labeled, as shown in Table 2.

2.3 Characterization

The proximate analysis, which includes estimation of moisture content, volatile matter, ash, and fixed carbon content, was carried out by using thermogravimetric analyzer (Eltra Thermostep). The ultimate analysis, which includes the evaluation of carbon, nitrogen, hydrogen, and sulfur content as weight percent, was performed by using the CHNS analyzer

(Vario Micro cube, Elementar). The surface area was measured by the BET surface area analyzer (Micromeritics, model ASAP 2020). The surface morphology/microstructures of the raw material and the ACs were examined using field emission scanning electron microscopy (FE-SEM Supra 55, Carl Zeiss). Identification and characterization of functional groups were made by using FTIR (Cary 660, Agilent Technologies).

2.4 Batch adsorption studies

A stock solution of methylene blue (MB) 1.0 g/L (1000 ppm) was prepared by dissolving 1 g of MB in double distilled water in a standard volumetric flask. Equilibrium adsorption experiments were performed by taking 100 ml of MB solutions in 250-ml conical flasks with various initial concentrations (20–200 mg/L) and at the natural pH of the solutions. A quantity of 0.1 g of AC was added to each flask and maintained at different constant temperatures (25 °C, 30 °C, and 40 °C) in an orbital incubator shaker at 150 rpm. The experiments were carried out for 24 h to guarantee that the equilibrium was attained. All samples were filtered before analysis, and the concentration of the samples before and after adsorption was determined using a UV–vis spectrophotometer (Thermo Fisher Evolution™ 300) at its maximum wavelength (λ) of 664 nm. Similar sets of experiments were repeated at the

Table 4 Proximate analysis of the raw material and prepared ACs

Sample	Moisture (wt.%)	Volatile matter (wt.%)	Ash (wt.%)	Fixed carbon (wt.%)
BR	5.88	72.83	3.14	18.16
AC-11-400	13.27	29.34	3.56	53.83
AC-12-400	13.88	29.08	3.29	53.75
AC-13-400	11.99	28.67	3.65	55.68
AC-14-400	12.06	29.26	3.20	55.48
AC-11-500	14.72	24.01	3.48	57.79
AC-12-500	13.49	22.41	2.41	61.69
AC-13-500	14.34	22.37	3.10	60.19
AC-14-500	11.06	24.30	3.39	61.26
AC-11-600	11.33	17.86	3.16	67.66
AC-12-600	11.07	18.17	2.29	68.48
AC-13-600	14.70	16.28	2.87	66.14
AC-14-600	12.68	18.79	2.90	65.63

Table 5 Ultimate analysis of the raw material and ACs

Sample	Carbonization temperature (°C)	C (wt.%)	H (wt.%)	N (wt.%)	S (wt.%)
BR	-	36.84	5.53	8.88	0.00
AC-11-400	400	54.35	3.67	0.91	0.09
AC-12-400		53.54	3.15	0.97	0.08
AC-13-400		59.79	3.91	1.02	0.07
AC-14-400		57.37	3.07	1.05	0.07
AC-11-500	500	53.12	3.94	0.83	0.31
AC-12-500		53.68	3.76	0.94	0.15
AC-13-500		51.65	3.87	0.84	0.18
AC-14-500		60.04	4.02	0.98	0.09
AC-11-600	600	60.12	1.90	0.74	0.00
AC-12-600		59.24	1.56	0.92	0.02
AC-13-600		63.57	1.74	0.99	0.06
AC-14-600		61.52	0.96	0.52	0.07

temperatures of 30 °C and 40 °C. Duplicate experiments were performed, and only the average values are reported. The amount of MB adsorbed onto activated carbon, q_e (mg/g), was calculated by the following equation.

$$q_e = \frac{(C_o - C_e)V}{W} \tag{1}$$

where C_o and C_e (mg/L) are the initial and equilibrium MB concentrations in the liquid phase, respectively, V (L) is the volume of the solution, and W (g) is the mass of dry adsorbent added.

For batch kinetic studies, 0.2 g of prepared AC was contacted with 200 ml of MB solutions of initial concentrations, 50, 100, 150, and 200 mg/L, for 12 h contact time and a temperature of 30 °C was employed. A similar set of experiments was conducted at a different temperature of 40 °C. The samples taken at regular time intervals were analyzed for MB concentration, as mentioned earlier. Using these concentration data, the amount of MB adsorbed at any time, q_t (mg/g), was calculated by the following equation.

$$q_t = \frac{(C_o - C_t)V}{W} \tag{2}$$

where C_t (mg/L) is the MB concentration at any time "t."

Table 6 BET surface area of the raw BR and a few ACs

Sample	BET surface area (m²/g)
BR	4
AC-14-400	830
AC-14-500	838
AC-11-600	654
AC-12-600	803
AC-13-600	894
AC-14-600	903

2.5 Adsorption isotherm models

The current study identifies the isotherm parameters based on the maximum value of the coefficient of determination and minimum value of error function to estimate the best-fit equilibrium isotherm model for the single solute system. The isotherm models such as Freundlich, Langmuir, and Temkin were investigated in the linear and non-linear forms to describe the equilibrium characteristics of MB adsorption onto prepared activated carbons (Table 3).

2.6 Kinetic models

For adsorption kinetic study, the concentration of the MB in the solution as a function of time was investigated using the Lagergren pseudo-first-order model (Eq. 3) [22] and Ho's pseudo-second-order model (Eq. 4) [23].

$$q = q_e\left(1 - e^{-k_1 t}\right) \tag{3}$$

$$q = \frac{q_e^2 k_2 t}{1 + q_e k_2 t} \tag{4}$$

where q_e is adsorption capacity at equilibrium (mg/g), q is the amount of MB adsorbed (mg/g) at time t, k_1 is the rate constant of pseudo-first-order sorption (1/min), and k_2 is the rate constant of pseudo-second-order sorption (g/mg min).

3 Results and discussion

3.1 Characterization of the raw material and the prepared activated carbons

The proximate and ultimate analyses of the banana root and the prepared ACs are shown in Tables 4 and 5, respectively.
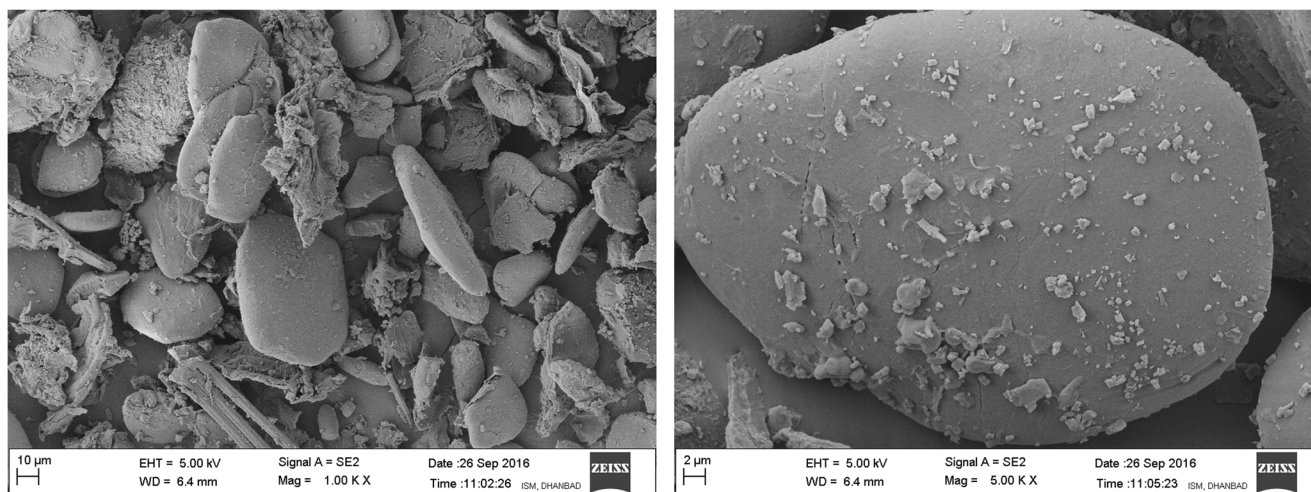
Fig. 1 FE-SEM images of the banana root (magnification: 1.00 KX and 5.00 KX)

The results show that the raw material has a high volatile matter and low ash content, thus making it a good starting material for the preparation of activated carbon [24]. The fixed carbon content of the prepared ACs is very high compared with that of the raw material.

The carbon content of the prepared ACs increases with an increase in the carbonization temperature from 400 to 600 °C due to an increasing degree of aromaticity [25]. The weight percentages of hydrogen, nitrogen, and oxygen of the prepared ACs decreased in comparison with the values for the raw material due to the decomposition of banana root (BR) as volatile compounds during the activation and carbonization processes.

The total BET surface area of the raw material and a few prepared ACs is shown in Table 6. The surface area of the raw material is shallow; however, it increased for the prepared ACs due to chemical activation and carbonization of the raw material. The raw material is having a surface area of 4 m²/g, while for the AC, the maximum surface area obtained was 903 m²/g. The surface area of the prepared ACs increased with an increase in the carbonization temperature. The increase in surface area is due to the escape of the volatile matter from the core of the material and an increase in the aromaticity.

Field emission scanning electron microscopy (FE-SEM) helps in the direct observation of the surface microstructures of the raw material and the prepared ACs. Figures 1 and 2 show the FE-SEM images of the banana root and the ACs developed under different conditions, as mentioned earlier, respectively. It could be observed that the surface of raw material was quite dense without any pores.

There are substantial modifications in the surface morphology of the banana root and the prepared ACs. After chemical activation and carbonization, the compact structure of the raw material turned to be porous. The pores on the activated carbons are due to the release of volatiles and the reaction between carbon and the chemical activating agent, resulting in the higher BET surface area of the ACs.

The FTIR spectra of the BR and some of the prepared ACs are shown in Fig. 3 and recorded within the range of 4000–400 cm^{-1}. Various functional groups present on the raw material and the prepared ACs present were hydroxyl, carboxylic, carbonyl, and phenol. The wavenumbers corresponding to different functional groups that were present in the materials are listed in Table 7.

The presence of a hydroxyl functional group ($O-H$) results in the raw material a broad peak between 3000 and 3900 wavenumber. It was attributed to an associated O–H stretching vibration in cellulose, hemicellulose, lignin, or adsorbed water. After the activation of the raw material, the broad peak was significantly reduced, indicating hydroxyl dehydration or evaporation of adsorbed water during the carbonization process [32]. The presence of these negatively charged functional groups listed in Table 7 in the prepared activated carbons makes them better adsorbents for the removal of cationic dyes.

3.2 Adsorption isotherms

An adsorption isotherm describes how solutes interact with the adsorbents. Equilibrium experimental data of adsorption of MB on the prepared ACs subjected to the linear and non-linear isotherm model-based regression analyses are shown in Figs. 4 and 5, respectively.

Figure 4 shows the linear isotherm plots for MB adsorption on the prepared activated carbons at three different temperatures 25 °C, 30 °C, and 40 °C obtained using the Origin Pro 9.1 software. The Langmuir's parameters Q_0 and K_L can be determined by plotting graph between C_e/q_e vs. C_e. Similarly, the Freundlich parameters K_F and $1/n$ are determined by plotting of $\ln q_e$ vs. $\ln C_e$ and graph between q_e vs. $\ln C_e$ helps to
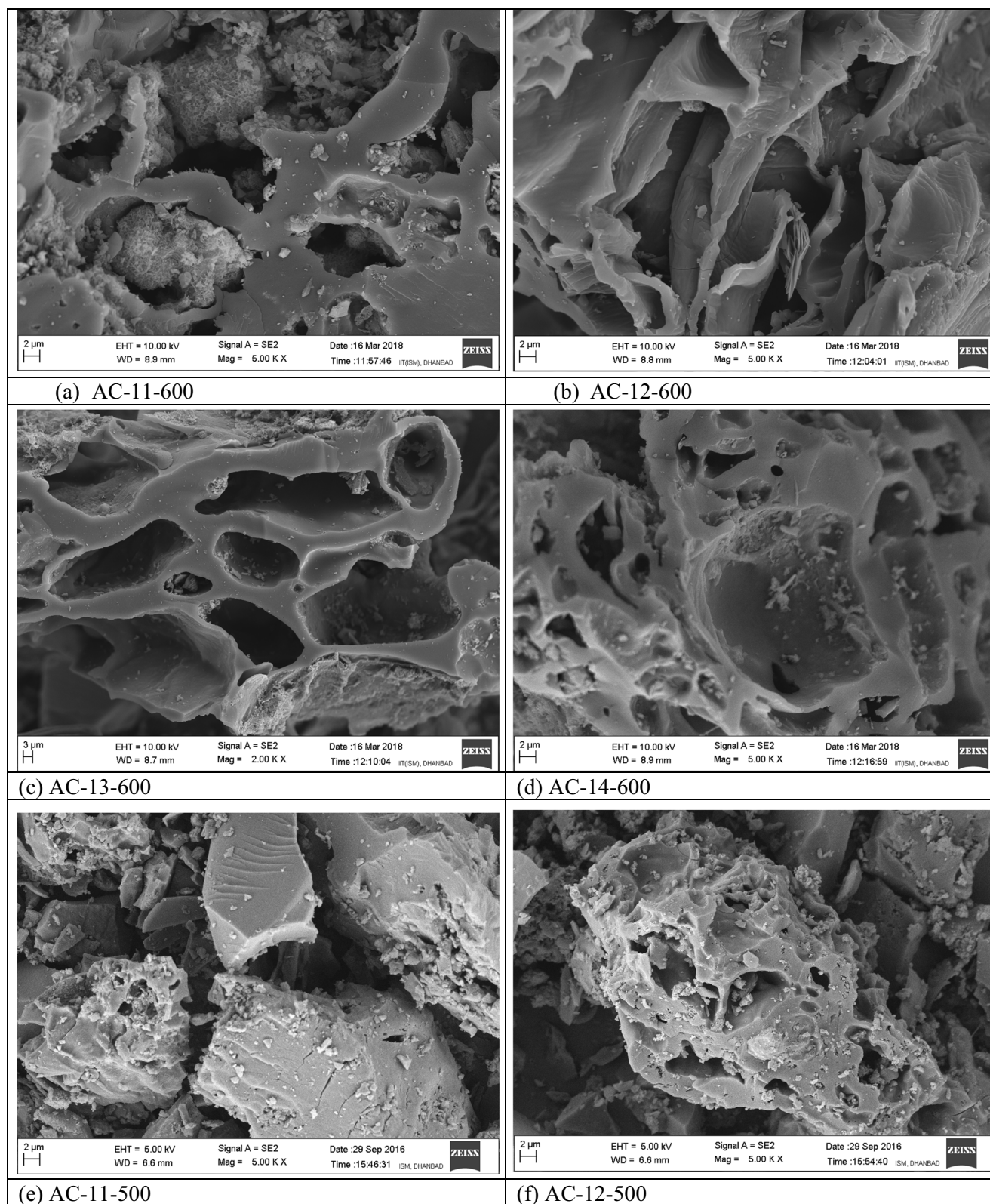
Fig. 2 FE-SEM images of ACs at different conditions. **a–d** At 600 °C, **e–h** at 500 °C, **i–l** at 400 °C (magnification: **a–h**: 5.00 KX and **i–l**: 1.00 KX)

calculate the Temkin parameters b_T and K_T. In Tables 8 and 9, linear adsorption isotherm parameters and values of the corresponding mentioned error functions are listed, respectively.

From Table 8, it is evident that the linear Langmuir model best fitted with the experimental data as the R^2 values are higher in comparison with the other models. However, the

(g) AC-13-500

(h) AC-14-500

(i) AC-11-400

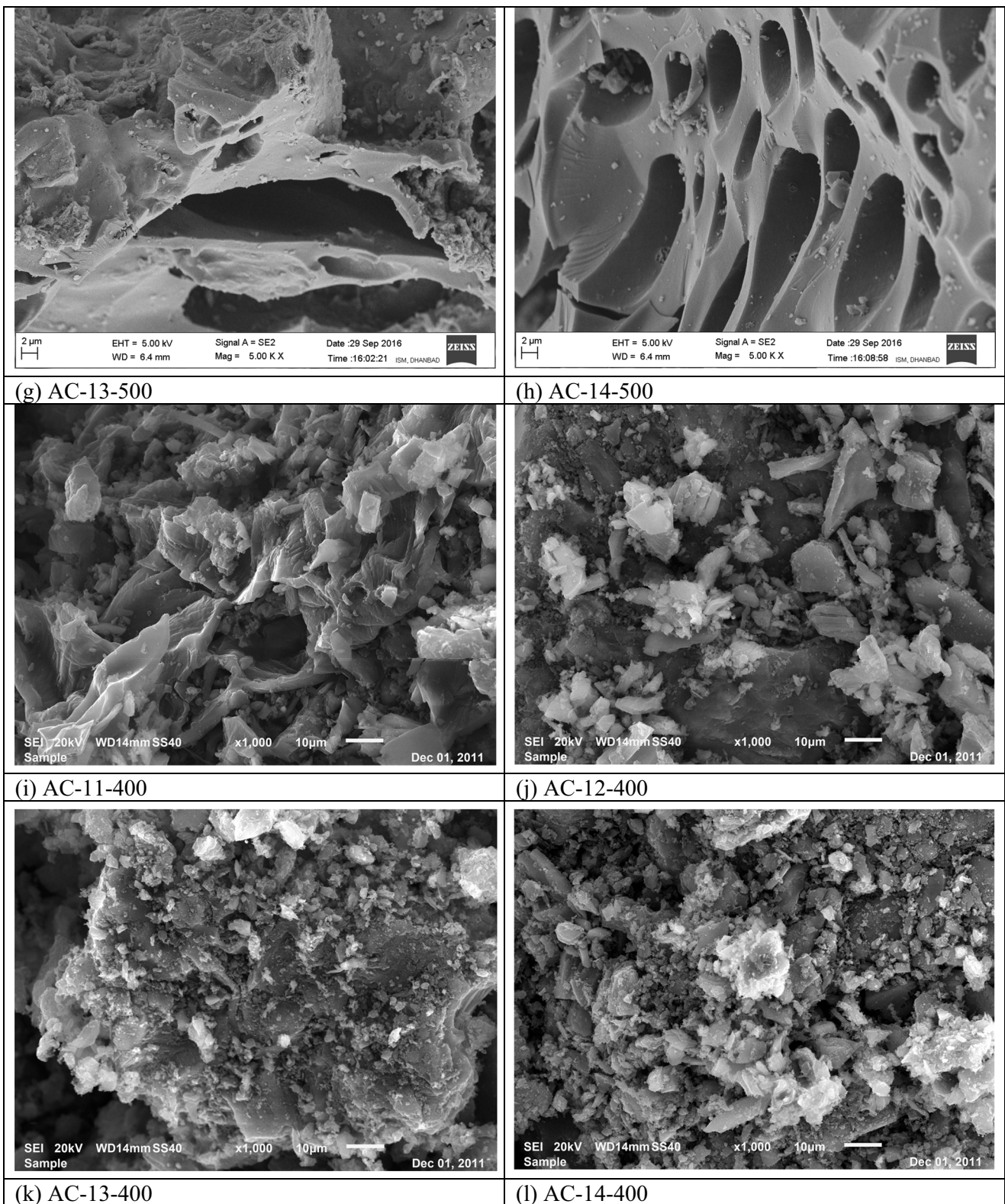(j) AC-12-400

(k) AC-13-400

(l) AC-14-400

Fig. 2 (continued)

predicted values of the linear Langmuir model are inconsistent with the experimental data at lower concentrations. From Table 9, it can be observed that the values of the error

functions are higher for the linear Langmuir model in comparison with the other two models. So, from Table 9, the Temkin isotherm model was the optimum isotherm, followed by
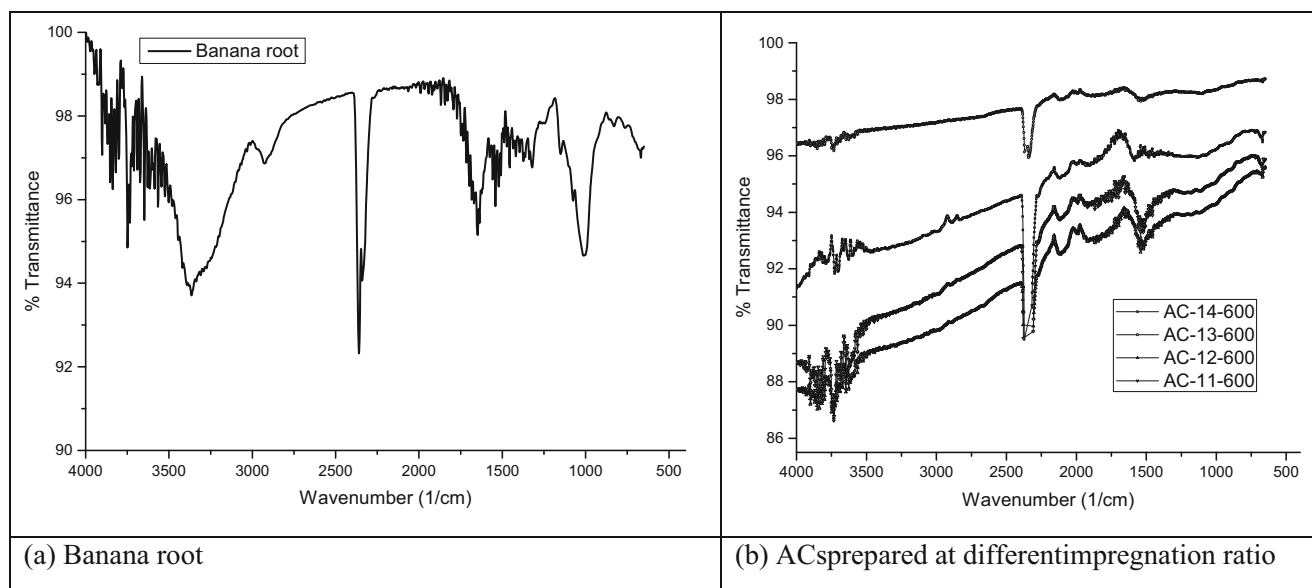
Fig. 3 FTIR spectra of the BR and a few prepared ACs

Freundlich and Langmuir isotherm for the linear method to describe the adsorption of MB on the prepared ACs.

The plots of C_e vs. q_e for different non-linear isotherm models with the experimental data were presented in Fig. 5. The parameters for various non-linear isotherms and values of the error functions were shown in Tables 10 and 11, respectively. The coefficient of determination (R^2) was used to assess the model's fitting with experimental data. As can be seen from Tables 10 and 11, the Temkin isotherm model is the most consistent with the experimental data, which is followed by Freundlich and Langmuir isotherm models based on the minimum value of the SSE and higher coefficient of determination. In both linear and non-linear forms, the Temkin model best fitted with the experimental data, followed by Freundlich and Langmuir.

It can be observed from Fig. 5 that, at a low concentration of the adsorbate, a sudden increase in the adsorption, this means that the adsorbate has a high affinity to the adsorbent. At a higher concentration of the adsorbate, the amount adsorbed per unit mass of the adsorbent increases slightly and becomes almost constant afterward. The adsorption capacity of adsorbents increased with an increase in

carbonization temperature from 400 to 600 °C, at any batch adsorption temperature. The high surface area of the prepared ACs makes them better adsorbents in the adsorption process. With an increase in the batch adsorption temperature, the adsorption also increased. The increase in temperature might increase the mobility of the dye particles; thereby, the interaction between the adsorbate and the active spots present on the adsorbent surface could upsurge, and also the adsorbent particle might swell with an increase in temperature [33]. Also, the adsorption capacity of the adsorbent was found to increase with an increase in the impregnation ratio. This might be due to the multilayer adsorption of methylene blue molecules onto the porous structure of the ACs. Similar trends were obtained in the fitting of the equilibrium data of adsorption of MB onto prepared ACs at carbonization temperatures of 500 °C and 400 °C, also, at the batch adsorption temperatures of 25 °C, 30 °C, and 40 °C.

The maximum adsorption capacity of the prepared ACs was found to be 139 mg/g, 142 mg/g, and 165 mg/g, respectively, at adsorption temperature of 25 °C, 30 °C, and 40 °C, for an initial MB concentration of 200 mg/L. Adsorption capacities for the removal of MB using the prepared ACs from

Table 7 Functional groups and corresponding wavenumbers

| Wavenumber (cm^{-1})	Peak (cm^{-1})	Functional group	Possible compounds	Reference
3300–3500	3364.84	$O-H$ stretching	Water, alcohol, phenols	[26]
2830–3000	2925.69	$C-H$ stretching	Alkanes	[27, 28]
1500–1845	1521.59, 1669.94	$C=O$ stretching $C=C$ stretching	Ketones, aldehydes, carboxylic acids	[29]
950–1300	1149.40	$C-O$ stretching	Esters, ethers	[30]
	1011.61	$O-H$ bending		
675–900	668.80	$C-H$ bending	Aromatic	[31]
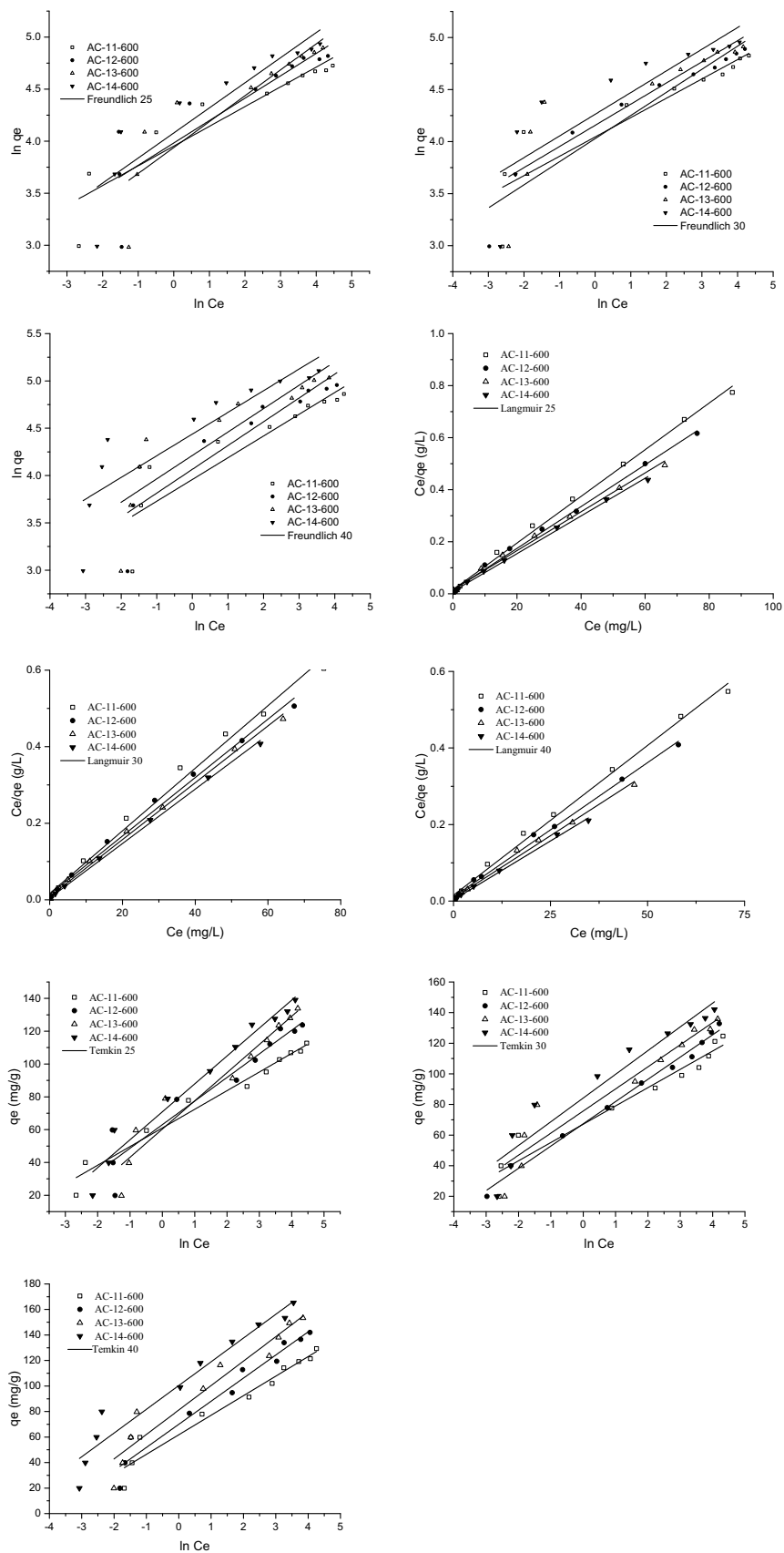
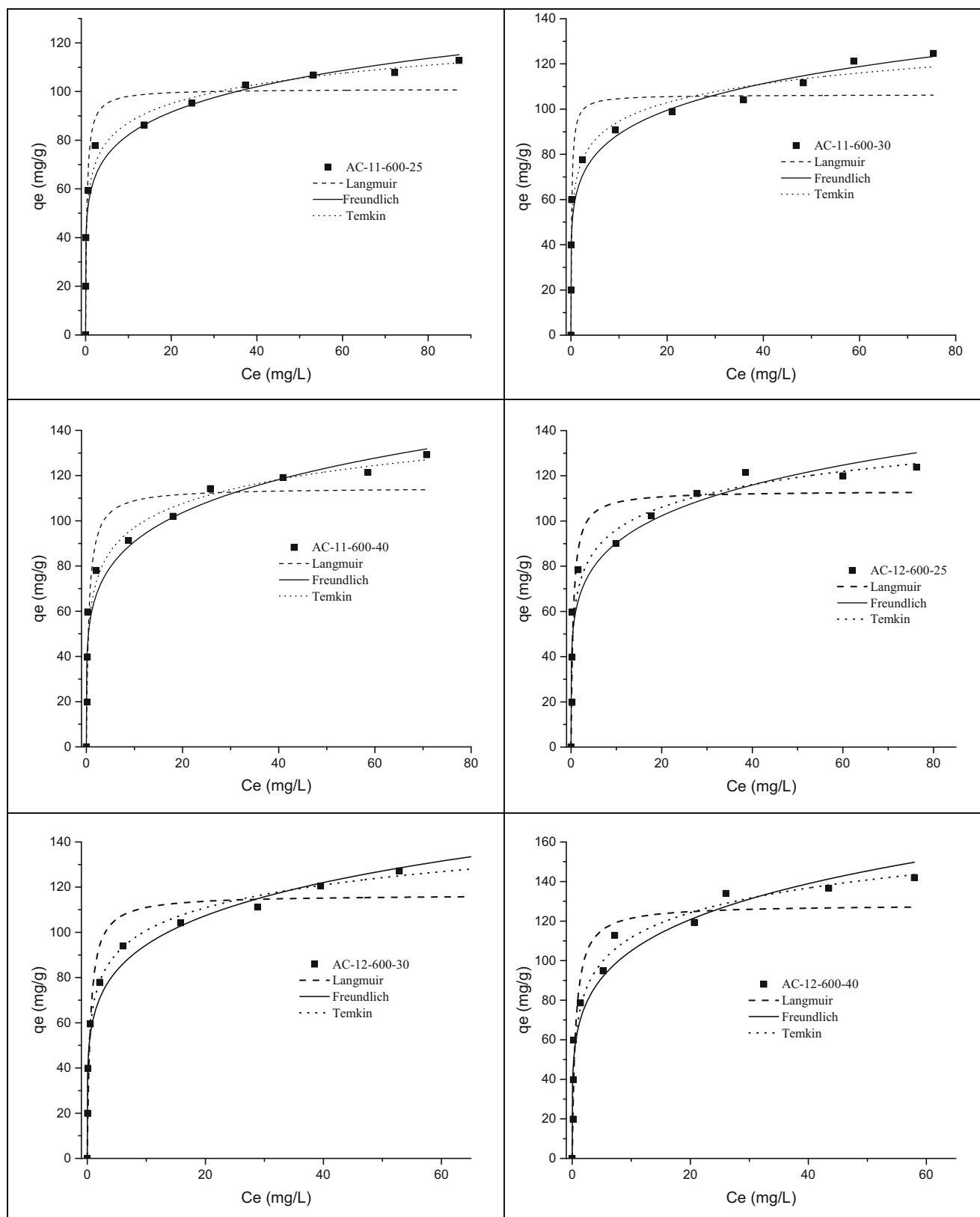**Fig. 4** Linear adsorption isotherms of ACs prepared at 600 °C

Fig. 5 Experimental data and non-linear isotherms at different adsorption temperatures of ACs prepared at 600 °C
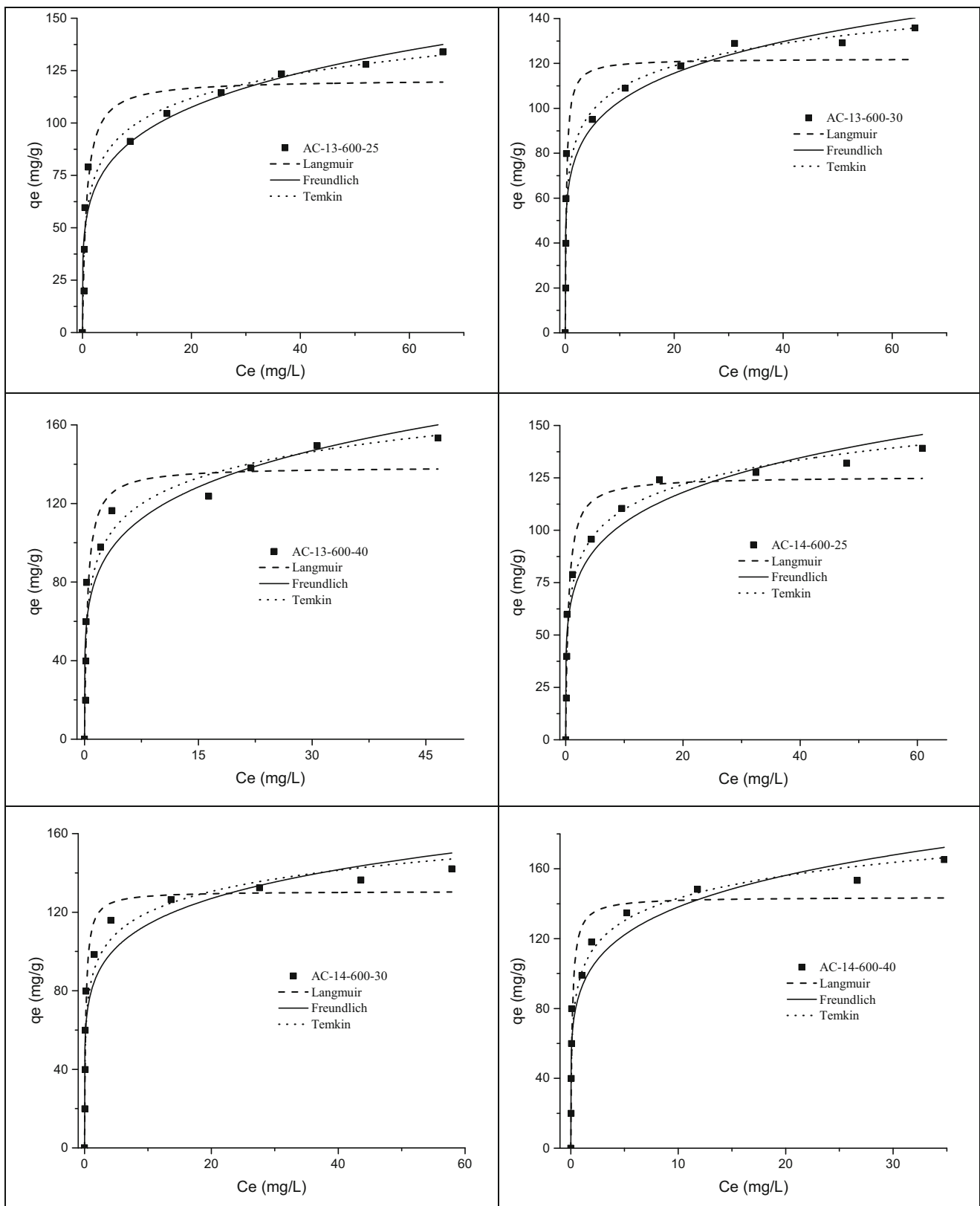
Fig. 5 (continued)

Table 8 Adsorption isotherm parameters obtained by linear regression analysis

Parameter	AC-11-600			AC-12-600		
	25 °C	30 °C	40 °C	25 °C	30 °C	40 °C
Langmuir						
Q_o	111.4827	122.2494	127.8772	124.5330	131.0616	142.4501
K_L	0.5735	0.4946	0.5085	0.5806	0.5438	0.6585
R^2	0.9966	0.9906	0.9952	0.9970	0.9932	0.9963
Freundlich						
K_F	52.0836	57.0912	52.3614	53.6655	56.1895	58.3016
n	5.2740	5.3824	4.3518	4.6512	4.5045	3.9787
R^2	0.8687	0.8230	0.8216	0.7640	0.9223	0.8241
Temkin						
b	217.9917	210.8813	169.8954	172.1143	173.4151	143.7138
k	214.3683	275.0423	56.4386	79.5928	103.2888	47.6698
R^2	0.9680	0.9314	0.9460	0.9049	0.9911	0.9514
	AC-13-600			AC-14-600		
Langmuir						
Q_o	133.8688	134.5895	152.9052	137.9310	140.6470	162.6016
K_L	0.4511	0.8570	0.9021	0.7804	1.5160	1.8580
R^2	0.9945	0.9971	0.9941	0.9975	0.9987	0.9972
Freundlich						
K_F	52.0836	57.0912	52.3614	53.6655	56.1895	58.3016
n	5.2740	5.3824	4.3518	4.6512	4.5045	3.9787
R^2	0.8687	0.8230	0.8216	0.7640	0.9223	0.8241
Temkin						
b	217.9917	210.8813	169.8954	172.1143	173.4151	143.7138
k	214.3683	275.0423	56.4386	79.5928	103.2888	47.6698
R^2	0.9680	0.9314	0.9460	0.9049	0.9911	0.9514

Table 9 Error functions obtained by the linear regression method

Parameter	AC-11-600			AC-12-600			AC-13-600			AC-14-600		
	25 °C	30 °C	40 °C	25 °C	30 °C	40 °C	25 °C	30 °C	40 °C	25 °C	30 °C	40 °C
Langmuir												
R^2	0.7696	0.7115	0.8039	0.7767	0.8328	0.8536	0.7993	0.7157	0.8209	0.8618	0.8120	0.8047
SSE	2841.2	4795.9	3144.6	3598.0	2730.6	2879.5	3564.8	6268.3	4415.4	2544.5	4111.1	5759.4
SAE	126.6	162.1	131.2	133.7	129.8	120.7	142.0	177.5	141.5	119.5	134.5	175.7
ARE	26.8	31.5	23.7	22.9	26.4	20.9	22.5	29.7	21.1	21.2	22.4	27.0
HYBRID	33.5	39.3	29.6	28.6	33.0	26.1	28.2	37.1	26.3	26.5	28.0	33.8
MPSD	45.9	52.7	38.8	38.5	45.5	35.2	34.9	46.5.5	35.1	34.7	37.4	42.6
Freundlich												
R^2	0.9188	0.9260	0.9122	0.8905	0.9472	0.8993	0.8975	0.8786	0.8636	0.8887	0.8362	0.8633
SSE	793.9	890.5	1208.6	1484.7	740.5	1854.3	1578.1	2042.7	3096.5	1953.7	3311.1	3634.0
SAE	71.4	72.4	88.7	94.3	80.3	117.4	91.9	108.1	156.5	126.8	165.2	165.9
ARE	155.7	216.6	251.1	337.9	118.9	315.5	320.8	386.4	500.9	297.8	509.7	534.1
HYBRID	194.6	270.8	313.8	422.4	148.6	394.4	401.0	483.0	626.1	372.2	637.1	667.7
MPSD	24.1	30.5	31.8	38.3	19.7	34.4	35.9	38.4	42.6	31.7	42.1	43.5
Temkin												
R^2	0.9724	0.9425	0.9542	0.9220	0.9921	0.9586	0.9395	0.9219	0.9316	0.9686	0.9289	0.9458
SSE	255.3	679.1	602.9	1020.4	105.2	715.4	889.5	1252.0	1438.5	505.7	1294.2	1315.6
SAE	39.0	62.5	53.5	70.4	26.4	62.4	66.1	77.1	91.5	52.6	94.3	82.9
ARE	9.7	14.1	13.0	17.7	5.0	14.1	16.1	18.5	20.1	12.2	20.7	19.1
HYBRID	12.1	17.6	16.3	22.1	6.2	17.6	20.1	23.1	25.1	15.2	25.9	23.9
MPSD	20.4	30.6	30.6	41.6	9.0	32.5	35.8	39.7	43.1	27.1	43.1	43.2

Table 10 Adsorption isotherm parameters obtained by non-linear regression analysis

Parameter	AC-11-600			AC-12-600		
	25 °C	30 °C	40 °C	25 °C	30 °C	40 °C
Langmuir						
Q_o	101.0471	106.3899	114.6246	113.341	116.6297	128.3115
K_L	3.2528	6.0164	1.9097	2.1124	1.9842	1.7710
R^2	0.9344	0.8950	0.9241	0.9022	0.9205	0.9219
Freundlich						
K_F	57.3936	61.3026	58.5406	59.6333	61.7427	65.8689
n	6.4183	6.1853	5.2471	5.5494	5.4147	4.9428
R^2	0.9593	0.9523	0.9487	0.9273	0.9782	0.9433
Temkin						
b	217.9917	210.8813	169.8953	172.1143	173.4151	143.7138
k	214.3679	275.0424	56.4385	79.5928	103.2887	47.6698
R^2	0.9809	0.9573	0.9656	0.9400	0.9943	0.9676
	AC-13-600			AC-14-600		
Langmuir						
Q_o	120.8165	122.1277	138.6782	125.6722	130.6991	143.8819
K_L	1.3913	4.4810	2.6101	2.1421	4.9528	7.2116
R^2	0.9323	0.9235	0.9277	0.9428	0.9519	0.9136
Freundlich						
K_F	58.1358	70.3494	75.8345	67.0414	79.1362	91.8428
n	4.8713	6.0271	5.1433	5.2933	6.3382	5.6387
R^2	0.9359	0.9197	0.9138	0.9433	0.9018	0.9201
Temkin						
b	144.0677	174.5966	135.8171	145.5356	168.0006	139.8171
k	33.3562	190.1655	69.1675	64.1474	229.6181	219.6901
R^2	0.9531	0.9379	0.9435	0.9760	0.9427	0.9548

different resources reported in the literature were compared with the present work in Table 12. The MB removal adsorption capacities of the ACs developed in this work are substantial in comparison with others.

3.3 Assessment of linear and non-linear methods

As shown from the previous tables, various isotherm parameters are obtained by different linear and non-linear models.

Table 11 Error functions obtained by non-linear regression method

Parameter	AC-11-600			AC-12-600			AC-13-600			AC-14-600		
	25 °C	30 °C	40 °C	25 °C	30 °C	40 °C	25 °C	30 °C	40 °C	25 °C	30 °C	40 °C
Langmuir												
R^2	0.9108	0.8695	0.9041	0.8788	0.9012	0.9057	0.9150	0.9055	0.9142	0.9283	0.9396	0.9012
SSE	880.6	1671.1	1332.2	1664.4	1460.9	1724.2	1284.2	1543.1	1839.2	1205.6	1085.9	2516.8
SAE	81.9	114.2	102.9	109.7	105.3	117.9	97.0	112.3	120.6	93.4	92.8	135.2
ARE	12.0	18.4	16.2	20.2	16.9	17.4	16.2	18.7	19.0	12.8	16.0	19.5
HYBRID	15.0	23.0	20.2	25.3	21.1	21.8	20.2	23.4	23.7	16.0	20.0	24.4
MPSD	17.9	28.1	23.9	36.1	26.3	24.5	29.0	30.3	32.4	17.6	27.3	33.0
Freundlich												
R^2	0.9426	0.9362	0.9331	0.9071	0.9707	0.9297	0.9191	0.9013	0.8992	0.9289	0.8839	0.9080
SSE	547.2	759.3	899.5	1236.5	400.5	1252.0	1215.8	1618.8	2194.9	1194.4	2219.2	2327.0
SAE	46.0	60.2	68.4	83.4	45.3	90.7	75.2	94.9	114.1	93.7	122.6	126.3
ARE	12.6	15.4	17.7	20.8	11.4	20.8	19.9	22.9	26.3	21.0	27.4	27.5
HYBRID	15.7	19.3	22.1	26.0	14.3	26.0	24.9	28.6	32.9	26.2	34.2	34.3
MPSD	32.6	37.5	41.7	48.2	28.3	47.3	46.9	50.6	58.7	45.6	59.6	61.5
Temkin												
R^2	0.9724	0.9425	0.9542	0.9220	0.9921	0.9586	0.9395	0.9219	0.9316	0.9686	0.9237	0.9275
SSE	255.3	679.1	602.9	1020.4	105.2	715.4	889.5	1252.0	1438.5	505.7	1402.4	1827.2
SAE	39.0	62.5	53.5	70.4	26.4	62.4	66.1	77.1	91.5	52.6	93.8	112.4
ARE	9.7	14.1	13.0	17.7	5.0	14.1	16.1	18.5	20.1	12.2	20.2	22.4
HYBRID	12.1	17.6	16.3	22.1	6.2	17.6	20.1	23.1	25.1	15.2	25.3	28.0
MPSD	20.4	30.6	30.6	41.6	9.0	32.5	35.8	39.7	43.1	27.1	41.0	48.2

Table 12 Maximum adsorption capacities of MB adsorbed by various adsorbents

Adsorbent resource	Experimental conditions			Adsorption capacity (mg/g)	Reference
	Dosage (g)	Temperature (K)	Volume (ml)		
Hazelnut shells	0.5	293	50	76.90	[34]
Sawdust-walnut	0.5	293	50	59.17	
Coconut coir	0.25	303	50	15.59	[35]
Banana root	0.1	313	100	165	Present work
Banana root	0.1	303	100	142	
Banana root	0.1	298	100	139	
Graphene	0.5	293	100	153.85	[36]
Bamboo-based AC	1	303	50	454.20	[37]

On comparing, it was found that the values of isotherm parameters (K_F, n) acquired by the linear methods are nearer to those obtained by the non-linear method for the Freundlich model. But in the case of the Langmuir model, the values of isotherm parameters (Q_0, K_L) acquired by the linear method are different from those obtained by the non-linear method.
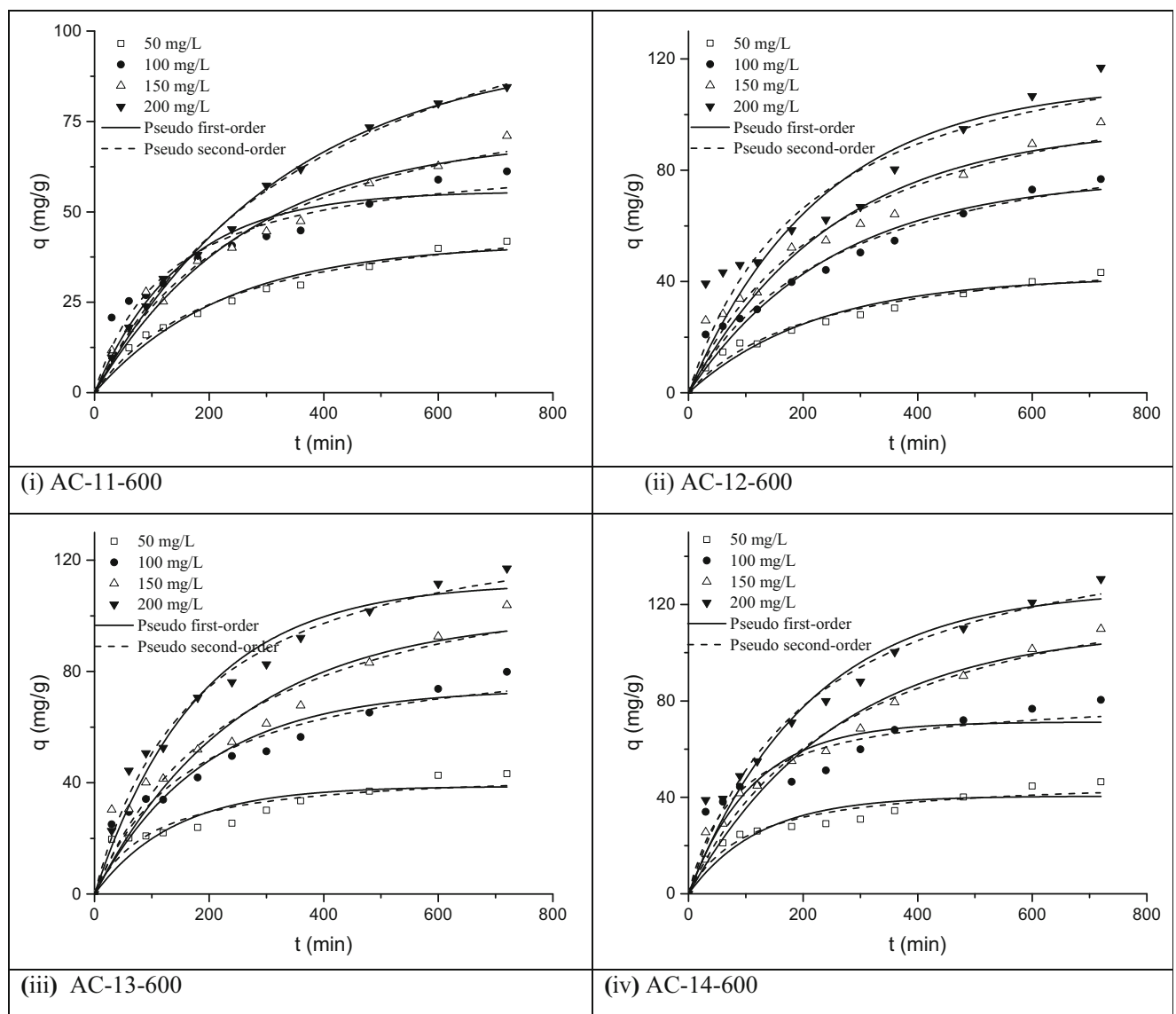

Fig. 6 Experimental data and adsorption kinetics of MB onto activated carbons at 30 °C

There is no difference in the value of isotherm parameters (K_T, b_T) acquired by the linear and non-linear method for the Temkin model because of its equation structure. In both linear and non-linear forms, the Temkin model best fitted with the experimental data, followed by Freundlich and Langmuir. The magnitudes of error functions in the non-linear model are lower than the linear model, which indicates that the non-linear method is the more appropriate method for the evaluation of adsorption isotherm parameters.

3.4 Kinetic studies

Four different initial concentrations of adsorbate, ranging from 50 to 200 mg/L with a difference of 50 mg/L, were taken for adsorption kinetic experiments. The non-linear pseudo-first-order and pseudo-second-order kinetic models were used to fit the adsorption kinetic experimental data. Experimental data at adsorption temperature of 30 °C and 40 °C and non-linear model-based curve fitting are shown in Figs. 6 and 7, respectively. Typical kinetic curves were observed, where a fast rate of adsorption was observed until 300 min, and after that, the rate of adsorption decreased; the kinetic equilibrium was attained at around 800 min. With an increase in contact time, the active sites available for adsorption decreased. The kinetic profile indicated that the adsorbate molecules progressively occupied the adsorbent surface. As the temperature was increased, the adsorption capacity increased, indicating that the adsorption was an endothermic process. The adsorption kinetic parameters are listed in Tables 13 and 14 for the adsorption temperature of 30 °C and 40 °C, respectively. It can be observed that R^2 values of pseudo-first-order and pseudo-second-order models were close to unity. However, the
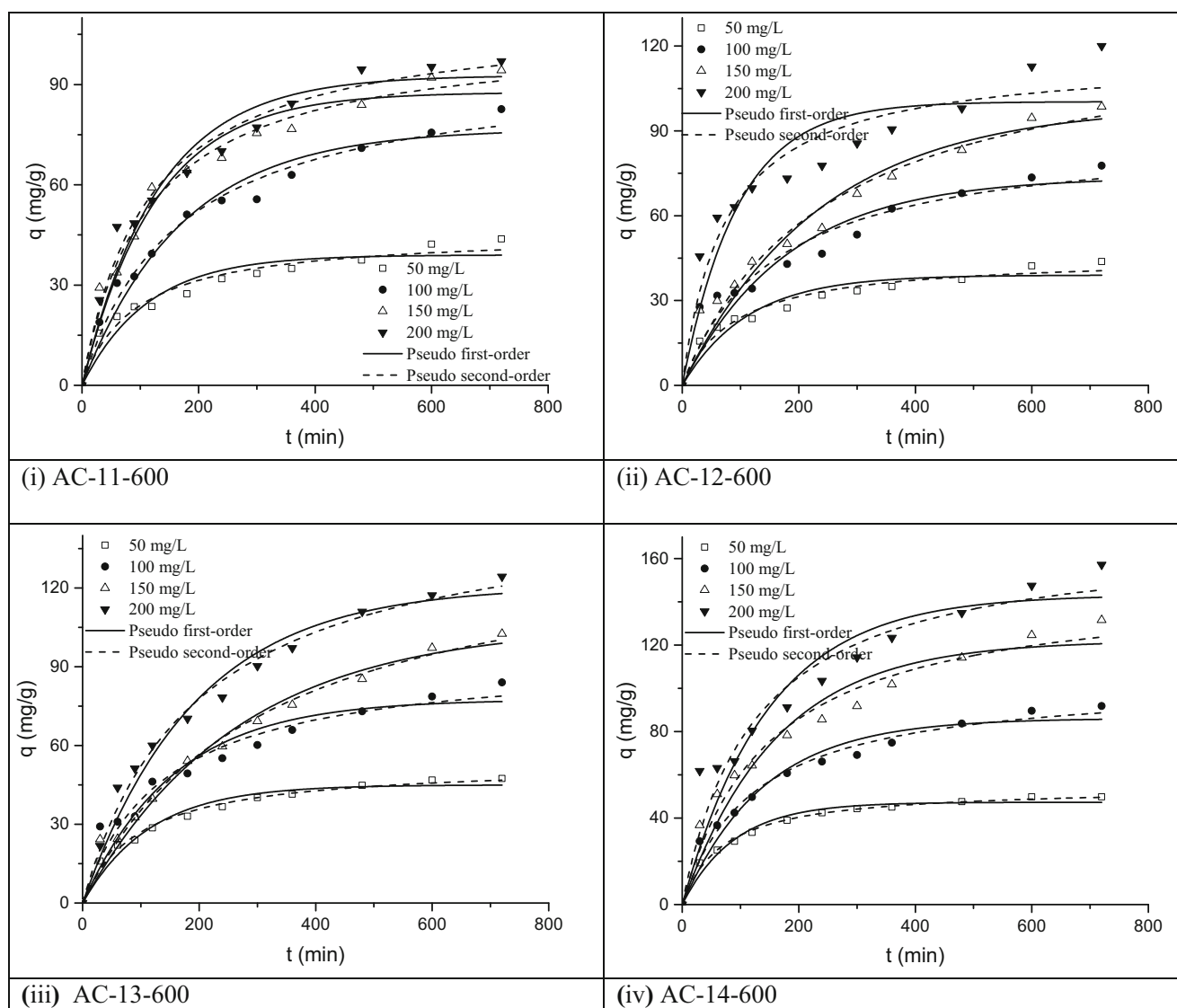

Fig. 7 Experimental data and adsorption kinetics of MB onto activated carbons at 40 °C

Table 13 Kinetic model parameters for the adsorption of MB on activated carbons at 30 °C

Adsorbent	Initial concentration (mg/L)	Pseudo-first order			Pseudo-second order		
		q_e (mg/g)	k_1 (min^{-1})	R^2	q_e (mg/g)	k_2 (g/mg/min)	R^2
AC-11-600	50	41.2	0.00442	0.9592	53.2	7.92674E-5	0.9758
	100	55.7	0.00665	0.9023	66.9	1.14997E-4	0.9452
	150	70.6	0.00377	0.9663	94.4	3.54249E-5	0.9781
	200	95.4	0.00299	0.9955	137.0	1.67788E-5	0.9965
AC-12-600	50	41.6	0.00449	0.9463	53.2	8.30757E-5	0.9675
	100	77.4	0.00401	0.9465	101.2	3.69685E-5	0.9619
	150	96.0	0.00393	0.9351	125.3	2.94014E-5	0.9531
	200	111.2	0.00431	0.8512	137.3	3.40621E-5	0.8862
AC-13-600	50	38.7	0.0072	0.7746	44.5	2.21008E-4	0.8498
	100	73.7	0.00525	0.8964	90.5	6.34725E-5	0.9325
	150	100.2	0.00399	0.9011	127.7	3.10378E-5	0.9264
	200	111.9	0.00553	0.9659	140.5	4.00262E-5	0.9844
AC-14-600	50	40.5	0.00809	0.8662	47.9	2.05095E-4	0.9278
	100	71.3	0.00895	0.8371	82.1	1.44854E-4	0.9077
	150	110.4	0.00386	0.9542	145.3	2.44254E-5	0.9689
	200	126.5	0.00473	0.9484	161.6	2.87481E-5	0.9661

pseudo-first-order model predicted data was closer to the experimental data and thus was more suitable for describing the adsorption kinetic process of the present study.

4 Conclusions

In this study, the banana root was used as the raw material, and zinc chloride was used as the chemical activation agent to derive ACs from biomass inexpensively. The precursor and all the prepared ACs have been characterized. Proximate and ultimate analyses were reported. The surface area, surface morphology, and different functional groups present were also reported. A maximum surface area of 903 m^2/g was observed for one of the prepared ACs. The prepared ACs were satisfactorily applied to the adsorption of MB in an aqueous solution. The amount of MB adsorbed increased with increased adsorption temperature, in agreement with an endothermic process. The adsorption capacity of the adsorbents increased with an increase in both impregnation ratio and carbonization

Table 14 Kinetic model parameters for the adsorption of MB on activated carbons at 40 °C

Adsorbent	Initial concentration (mg/L)	Pseudo-first order			Pseudo-second order		
		q_e (mg/g)	k_1 (min^{-1})	R^2	q_e (mg/g)	k_2 (g/mg/min)	R^2
AC-11-600	50	39.0	0.00892	0.9072	45.7	2.41314E-4	0.9579
	100	76.7	0.00585	0.9587	95.5	6.35115E-5	0.9806
	150	87.7	0.0079	0.9602	105.5	8.39734E-5	0.9829
	200	92.7	0.00768	0.9535	110.8	7.99655E-5	0.9802
AC-12-600	50	39.0	0.00892	0.9072	45.7	2.41314E-4	0.9579
	100	73.6	0.00552	0.8907	89.6	6.90385E-5	0.9248
	150	98.9	0.00424	0.9506	128.3	3.13706E-5	0.9663
	200	100.3	0.01051	0.8457	116.3	1.14615E-4	0.9205
AC-13-600	50	45.0	0.0087	0.9629	53.1	1.95452E-4	0.9886
	100	77.5	0.00641	0.9216	94.1	7.60787E-5	0.9542
	150	105.9	0.00379	0.9762	142.8	2.30006E-5	0.9838
	200	120.7	0.00521	0.9748	153.3	3.35532E-5	0.9893
AC-14-600	50	47.3	0.01126	0.9718	54.4	2.64834E-4	0.9943
	100	86.1	0.0072	0.9524	103.8	7.82795E-5	0.9805
	150	122.0	0.00619	0.9379	149.0	4.57319E-5	0.9699
	200	143.2	0.00677	0.8904	170.9	4.68395E-5	0.9332

temperature. The adsorption equilibrium data were fitted using linear and non-linear forms of isotherms, namely Langmuir, Freundlich, and Temkin models. Six different error functions were used to get the optimum isotherm and isotherm parameters. In comparison with the linear method, the non-linear method has a higher coefficient of determination and lower values of other error functions. The Temkin model was best suited to the experimental data.

In conclusion, the non-linear approach is a better way to estimate precisely the isotherm parameters. Non-linear pseudo-first-order and pseudo-second-order kinetic models were fitted to the experimental kinetic data. The pseudo-first-order model was found to be more suitable to describe the kinetic process.

References

1. Yagub MT, Sen TK, Afroze S, Ang HM (2014) Dye and its removal from aqueous solution by adsorption: a review. Adv Colloid Interf Sci 209:172–180. https://doi.org/10.1016/j.cis.2014.04.002

2. Davarnejad R, Afshar S, Etehadfar P (2020) Activated carbon blended with grape stalks powder: properties modification and its application in a dye adsorption. Arab J Chem Article in press 13: 5463–5473. https://doi.org/10.1016/j.arabjc.2020.03.025

3. Abhishek A, Chandi P, Senthilmurugan S, Selvaraju N (2020) Packed bed column studies of hexavalent chromium adsorption by zinc chloride activated carbon synthesized from Phanera vahlii fruit biomass. J Environ Chem Eng 8(4):103825. https://doi.org/10.1016/j.jece.2020.103825

4. Ghosh D, Bhattacharyya KG (2002) Adsorption of methylene blue on kaolinite. Appl Clay Sci 20:295–300. https://doi.org/10.1016/S0169-1317(01)00081-3

5. Aichour A, Zaghouane-Boudiaf H, Zuki FBM, Aroua MK, Ibbora CV (2019) Low-cost, biodegradable and highly effective adsorbents for batch and column fixed bed adsorption processes of methylene blue. J Environ Chem Eng 7:103409. https://doi.org/10.1016/j.jece.2019.103409

6. Pathania D, Sharma S, Singh P (2017) Removal of methylene blue by adsorption onto activated carbon developed from Ficus carica bast. Arab J Chem 10:S1445–S1451. https://doi.org/10.1016/j.arabjc.2013.04.021

7. Tasrin S, Mohamed Madhar Fazil S, Padmanaban VC, Selvaraju N Surface modification of nanocellulose using polypyrrole for the adsorptive removal of Congo red dye and chromium in binary mixture. Int J Biol Macromol 151:322–332. https://doi.org/10.1016/j.ijbiomac.2020.02.181

8. Shahnaz T, Sharma V, Subbiah S, Narayanasamy S. Multivariate optimisation of Cr (VI), Co (III) and Cu (II) adsorption onto nanobentonite incorporated nanocellulose/chitosan aerogel using response surface methodology. J Water Process Eng 36. https://doi.org/10.1016/j.jwpe.2020.101283

9. Saleem J, Shahid UB, Hijab M, Mackey H, McKay G (2019) Production and applications of activated carbons as adsorbents from olive stones. Biomass Convers Bioref 9:775–802. https://doi.org/10.1007/s13399-019-00473-7

10. Belhachemi M, Addoun F (2011) Comparative adsorption isotherms and modeling of methylene blue onto activated carbons. Appl Water Sci 1:111–117. https://doi.org/10.1007/s13201-011-0014-1

11. Kumar KV, Porkodi K (2006) Relation between some two- and three-parameter isotherm models for the sorption of methylene blue onto lemon peel. J Hazard Mater 138:633–635. https://doi.org/10.1016/j.jhazmat.2006.06.078

12. Vasanth Kumar K, Sivanesan S (2006) Isotherm parameters for basic dyes onto activated carbon: comparision of linear and non-linear method. J Hazard Mater 129:147–150. https://doi.org/10.1016/j.jhazmat.2005.08.022

13. Kumar KV, Porkodi K, Rocha F (2008) Isotherms and thermodynamics by linear and non-linear regression analysis for the sorption of methylene blue onto activated carbon: comparison of various error functions. J Hazard Mater 151:794–804. https://doi.org/10.1016/j.jhazmat.2007.06.056

14. Ncibi MC (2008) Applicability of some statistical tools to predict optimum adsorption isotherm after linear and non-linear regression analysis. J Hazard Mater 153:207–212. https://doi.org/10.1016/j.jhazmat.2007.08.038

15. Srenscek-Nazzal J, Narkiewicz U, Morawski AW, Wrobel RJ, Michalkiewicz B (2015) Comparison of optimized isotherm models and error functions for carbon dioxide adsorption on activated carbon. J Chem Eng Data 60:3148–3158. https://doi.org/10.1021/acs.jced.5b00294

16. Lim LBL, Namal P, Tennakoon DTB, Chieng HI, KhairudDahri M, Suklueng M (2017) Breadnut peel as a highly effective low-cost biosorbent for methylene blue: equilibrium, thermodynamic and kinetic studies. Arab J Chem 10:S3216–S3228. https://doi.org/10.1016/j.arabjc.2013.12.018

17. Mallakpour S, Tabesh F (2019) Tragacanthgum based hydrogel nanocomposites for the adsorption of methylene blue: comparison of linear and non-linear forms of different adsorption isotherm and kinetics models. Int J Biol Macromol 133:754–766. https://doi.org/10.1016/j.ijbiomac.2019.04.129

18. Allen SJ, Gan Q, Matthews R, Johnson PA (2003) Comparison of optimised isotherm models for basic dye adsorption by kudzu. Bioresour Technol 88(2):143–152. https://doi.org/10.1016/S0960-8524(02)00281-X

19. Kumar KV, Sivanesan S (2007) Isotherms for malachite green onto rubber wood (Heveabrasiliensis) sawdust: comparison of linear and non-linear methods. Dyes Pigments 72:124–129. https://doi.org/10.1016/j.dyepig.2005.07.021

20. Chan LS, Cheung WH, Allen SJ, McKay G (2012) Error analysis of adsorption isotherm models for acid dyes onto bamboo derived activated carbon. Chin J Chem Eng 20(3):535–542. https://doi.org/10.1016/S1004-9541(11)60216-4

21. Nebaghe KC, El Boundati Y, Ziat K, Naji A, Rghioui L, Saidi M (2016) Comparison of linear and non-linear method for determination of optimum equilibrium isotherm for adsorption of copper (II) onto treated Martil sand. Fluid Phase Equilib 430:188–194. https://doi.org/10.1016/j.fluid.2016.10.003

22. Lagergren SY (1898) Zur Theorie der sogenannten Adsorption gelöster Stoffe. https://doi.org/10.1007/BF01501332

23. Ho YS (1995) Absorption of heavy metals from waste streams by peat. University of Birmingham

24. Tien PD, Morisaka H, Satoh T, Miura M, Nomura M, Matsui H, Yamaguchi C (2003) Efficient evolution of hydrogen from tetrahydronaphthalene upon palladium catalyst supported on activated carbon fiber. Energy Fuel 17:658–660. https://doi.org/10.1021/ef020187a

25. Kumar A, Jena HM (2015) High surface area microporous activated carbons prepared from Fox nut (Euryale ferox) shell by zinc

chloride activation. Appl Surf Sci 356:753–761. https://doi.org/10.1016/j.apsusc.2015.08.074

26. Yang K, Peng J, Srinivasakannan C, Zhang L, Xia H, Duan X (2010) Preparation of high surface area activated carbon from coconut shells using microwave heating. Bioresour Technol 101:6163–6169. https://doi.org/10.1016/j.biortech.2010.03.001

27. Pradhan BK, Sandle NK (1999) Effect of different oxidizing agent treatments on the surface properties of activated carbons. Carbon 37:1323–1332. https://doi.org/10.1016/S0008-6223(98)00328-5

28. Ajmani A, Shahnaz T, Subbiah S, Narayanasamy S Hexavalent chromium adsorption on virgin, biochar, and chemically modified carbons prepared from Phanera vahlii fruit biomass: equilibrium, kinetics, and thermodynamics approach. Environ Sci Pollut Res 26(31):32137–32150. https://doi.org/10.1007/s11356-019-06335-z

29. Khelifi A, Almazán-Almazánb MC, Pérez-Mendoza M, Domingo-García M, López-Domingo FJ, Temdrara L, López-Garzón FJ, Addoun A (2010) Influence of nitric acid concentration on the characteristics of active carbons obtained from a mineral coal. Fuel Process Technol 91:1338–1344. https://doi.org/10.1016/j.fuproc.2010.05.004

30. Das D, Samal DP, Meikap BC (2015) Preparation of activated carbon from green coconut shell and its characterization. J Chem Eng Process Technol 6:1000248. https://doi.org/10.4172/2157-7048.1000248

31. Sugumaran P, Priya Susan V, Ravichandran P, Seshadri S (2012) Production and characterization of activated carbon from banana empty fruit bunch and Delonix regia fruit pod. J Sustain Energy Environ 3:125–132

32. Guo Y, Rockstraw DA (2007) Activated carbons prepared from rice hull by one-step phosphoric acid activation. Microporous Mesoporous Mater 100:12–19. https://doi.org/10.1016/j.micromeso.2006.10.006

33. Somsesta N, Sricharoenchaikul V, Aht-Ong D (2020) Adsorption removal of methylene blue onto activated carbon/cellulose biocomposite films: equilibrium and kinetic studies. Mater Chem Phys J 240:122221. https://doi.org/10.1016/j.matchemphys.2019.122221

34. Ferrero F (2007) Dye removal by low-cost adsorbents: hazelnut shells in comparison with wood sawdust. J Hazard Mater 142:144–152

35. Sharma YC, Uma, Upadhyay SN (2009) Removal of a cationic dye from wastewaters by adsorption on activated carbon developed from coconut coir. Energy Fuel 23:2983–2988

36. Liu TH, Li YH, Du QJ (2012) Adsorption of methylene blue from aqueous solution by graphene. Colloids Surf B Biointerfaces 90:197–203

37. Hameed BH, Din ATM, Ahmad AL (2007) Adsorption of methylene blue onto bamboo-based activated carbon: kinetics and equilibrium studies. J Hazard Mater 141:819–825

Publisher's Note Springer Nature remains neutral with regard to jurisdictional claims in published maps and institutional affiliations.